ELSEVIER

European Polymer Journal 39 (2003) 617–625

EUROPEAN POLYMER JOURNAL

www.elsevier.com/locate/europolj

# Cure behavior of epoxy resin/montmorillonite/imidazole nanocomposite by dynamic torsional vibration method

Xu Weibing [a,b], He Pingsheng [a,*], Chen Dazhu [a]

[a] *Department of Polymer Science and Engineering, University of Science and Technology of China, Hefei, Anhui 230026, China*
[b] *Department of Polymer Science and Engineering, Hefei University of Technology, Hefei, Anhui 230026, China*

Received 7 January 2002; received in revised form 20 September 2002; accepted 20 September 2002

**Abstract**

Flory's gelation theory, the non-equilibrium thermodynamic fluctuation theory and the Avrami equation have been used to predict the cure behavior of epoxy resin/organo-montmorillonite (Org-MMT)/imidazole intercalated nanocomposites at various temperatures and Org-MMT loadings. The theoretical prediction is in good agreement with the experimental results obtained by a dynamic torsional vibration method. The results show that the addition of Org-MMT reduces the gelation time $t_g$ and increases the rate of the curing reaction, the value of the kinetic constant $k$. The half-time $t_{1/2}$ of cure after the gel point decreases with increasing of cure temperature, and the value of $n$ is around 3 at lower temperature (<90 °C) and decreases to ~2 as the temperature increases. The addition of Org-MMT has no obvious effect on the apparent activation energy of the cure reaction. There is no special curing process required for the formation of an epoxy resin/Org-MMT/imidazole intercalated nanocomposite.


*Keywords:* Epoxy resin; Montmorillonite; Nanocomposite; Cure; Gel time; Avrami equation

## 1. Introduction

Composite materials, in which inorganic filler is dispersed within the polymer matrix on a nanometer scale, are called nanocomposites. One efficient approach to preparing such nanocomposites is in situ polymerization of monomer in the layered-silicate galleries [1,2]. In general, the dispersion of clay particles in a polymer matrix can result in the formation of three general types of composite materials: (a) conventional composites, (b) intercalated composites formed by the insertion of polymer into the clay host galleries (although the basal spacing rises, the clay remains in a regular gallery structure), (c) exfoliated nanocomposite, in which the individual 1 nm thick silicate layers are dispersed in a polymer matrix and segregated from one another, and the gallery structures are completely destroyed.

Recently, much attention has been paid to the layered silicate–epoxy nanocomposites, principally because of the far-ranging application potential of epoxy resin in many fields. Beyond some properties such as the excellent flame-retardant [3] and dielectric properties [4], the dramatic improvement of mechanical properties of this type of nanocomposite was discovered. Giannelis [5] prepared exfoliated layered silicate–epoxy nanocomposite from the diglycidyl ether of bisphenol-A and nadic methyl anhydride as curing agent, and found that the dynamic storage modulus of the nanocomposites containing 4% (by volume) silicate was approximately 58% higher in the glassy region and 450% higher in the rubbery plateau region compared to the pristine polymer. Monolithic epoxy exfoliated-clay nanocomposites have been prepared from the reaction of alkylammonium-exchanged smectite clays with the diglycidyl ether

* Corresponding author.
*E-mail address:* hpsm@ustc.edu.cn (P.S. He).

0014-3057/02/$ - see front matter 
PII: S0014-3057(02)00270-7

of bisphenol-A and *m*-phenylenediamine (MPDA) as the curing agent by Pinnavaia and his coworkers [6–8]. They found that the monolithic exfoliated clay nanocomposite could be formed by pre-swelling alkylammonium ion exchanged forms of the clays with epoxy resin prior to curing, and a tremendous improvement in tensile strength and modulus was realized, particularly when the resin matrix exhibited a subambient glass transition temperature. For instance, the reinforcement provided by the silicate layers at 16% (by weight) loading was manifested by more than 10-fold improvements in both tensile strength and modulus.

The nature and mechanism of the exfoliation process of the surface modified layered-silicate nanoparticles in the crosslinking epoxy network have been of recent interest. Lan [8] demonstrated that the exfoliation of the clay is not only dependent on the reactivity of the epoxy system but also on the rate of intercalation of epoxy and curing agent. Kornmann [2] compared the effect of aliphatic diamine and cycloaliphatic diamines on the structure of a nanocomposite, finding that although the former gave the slowest cure rate it allowed more curing agent to penetrate the epoxy swollen galleries and initiate intragallery polymerization leading to better exfoliation, which may be attributed to its characteristic of a more highly flexible backbone than the cycloaliphatic ones. Russell [9] found that for the MPDA cured epoxy systems, exfoliated nanocomposites were formed with epoxy cured with less than an equalmolar concentration of MPDA or with auto-polymerization of the epoxy without curing agent, whereas the intercalated structure was only observed with too much curing agent. This indicated that excessive curing agent resulted dominantly in the rapid rate of extragallery crosslinking in comparison to the slower intragallery diffusion, which suppressed the exfoliation. All of these publications about epoxy-clay nanocomposites concentrated on their formation mechanism, structure, as well as induced applied properties. However, no report, to the authors' knowledge could be found on the cure process in situ of the nanocomposite formation in the literature.

Curing of a resin system is the critical and productivity controlling step in the fabrication of thermosetting-matrix composites. However, the cure process of an epoxy resin is the crosslinking of linear macromolecules with a complicated mechanism. As soon as the crosslinking forms, the resin will not be softened and melted, leading to a difficulty to study. Traditionally, chemical analysis, Fourier transformed infrared spectroscopy [10] and differential scanning calorimetry [11,12] detecting the degree of conversion of reactive groups were used to study the cure process. The sensitivity and function of these analysis techniques are much reduced at the last curing stage due to the increased consumption of reactive groups. The cure process can be studied successfully by mechanical methods, and the dynamic torsional vibration method (DTVM) developed in our lab has successfully been used to investigate the cure behavior of the epoxy resin-$BF_3$-MEA system [13] and the epoxy resin-triethanolamine system [14]. In this paper, the intercalated nanocomposite was prepared via mixing epoxy resin with the desired amount of clay exchanged with alkylammonium bromide and with imidazole as curing agent. The isothermal cure process was monitored in situ by the DTVM, and Flory's gelation theory, the non-equilibrium thermodynamic fluctuation theory and the Avrami equation were used to analyze and predict the cure behavior of the epoxy resin/organo-montmorillonite (Org-MMT)/imidazole nanocomposite.

## 2. Experimental

### 2.1. Materials

$Na^+$-montmorillonite with a cation exchange capacity value of about 100 mmol/100 g was purchased from the Qingshan Chemistry Agent Factory in Lin'an, China. The diglycidyl ether of biphenyl A, epoxy resin E-51 with an epoxy value 0.48–0.54 and average epoxy equivalent 196, was obtained from the Shanghai Resin Factory. Imidazole was used as curing agent. The surfactant of clay, $(CH_3)_3(CH_2)_{16}NH_4Br$, was purchased from the Research Institute of Xinhua Active Material in Changzhou, and preparation of Org-MMT by ion exchange was carried out according to our previous paper [15]. For the isothermal cure experiment, the epoxy resin and the curing agent were mixed in the stoichiometric ratio of 100 parts resin to four parts curing agent (by weight). Then, the mixture was mixed with Org-MMT powder with loadings of 0, 5 and 10 phr, respectively.

### 2.2. Dynamic torsional vibration method and experimental curve

Dynamic torsional vibration is a non-resonant forced vibration [13]. The schematic diagram of a homemade experimental setup— HLX-I Resin Curemeter is shown in Fig. 1. The lower mold **3** having a heater within it and used as the torsional vibrator is filled with the resin materials. When the motor **6** is switched on, the upper mold **2** having a heater within it too comes down, and the molds close with a gap that can be adjusted. The cure temperature is controlled with thermistors. Thus, the isothermal cure process can be performed. As soon as the upper and lower molds close, the motor **5** is on, and the lower mold starts a torsional vibration with a frequency of 0.05 Hz at an angle below 1°, which also can be adjusted according to the hardness of cured resin

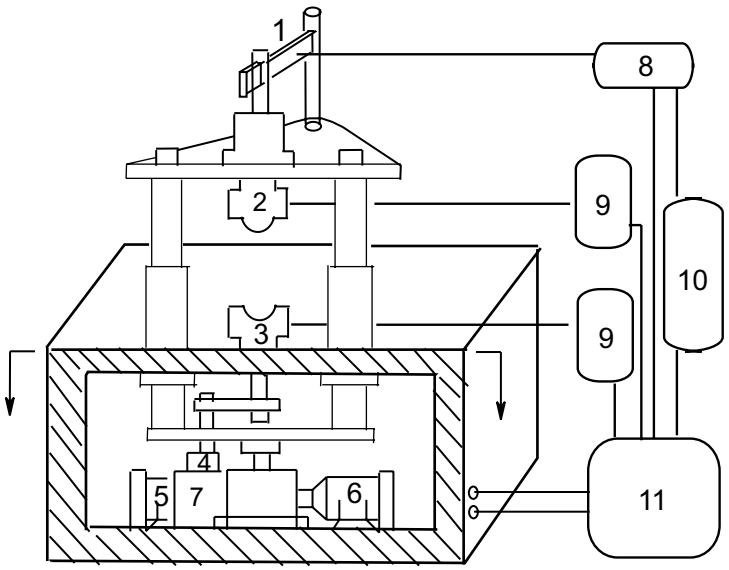


Fig. 1. Schematic representation of the dynamic torsional vibration apparatus. (1) Strain gauge load cell; (2) upper mold; (3) lower mold; (4) eccentric disc; (5) motor for torsional vibration; (6) motor for closing molds; (7) speed change gear; (8) amplifier; (9) temperature controller; (10) recorder; (11) power supporter.

materials, by means of an eccentric disc **4** on the speed change gear **7**. The torque amplitude of the torsional vibration is transformed into electric signals by means of the strain gauge load cell **1**, amplified through the amplifier **10** and recorded by the recorder **11**.

The resin system with a different degree of cure has a different torque (or modulus, viscosity etc.). Therefore, the change in the mechanical properties, i.e. the degree of cure of the resin system, can be monitored and determined by measuring the changes in torque, and a continuous curve reflecting the whole cure process can be obtained. A typical experimental curve obtained by DTVM is shown in Fig. 2. The abscissa is the curing time and the ordinate is the torque required to turn the resin system by a small angle, which corresponds to the modulus or viscosity of the resin system, and can be thought of as a relative parameter of the degree of cure. The time of closure of the molds is taken as the starting time of cure point O. In the range OA of the curing time the network structure formed during the cure reaction is not enough to cause forced vibration of the upper mold. As a result, the strain gauge load cell will not have any signal to input, so that the experimental curing curve is a linear line corresponding to the abscissa. At the point A, the viscosity of the resin system is high enough (i.e., the network formed is completed enough) for the gelation in the resin system to occur, and the torque appears and the strain gauge load cell inputs some signal. Thus, the point A is the gel point and the time corresponding to OA is the gel time $t_g$ for the system. After point A the torque increases with increasing curing time. The increasing amplitude of the torque (slope of the curve) reflects the rate of the curing reaction. The increasing trend of the torque tends to steady with increasing curing time, and the equilibrium torque $G_\infty$ is thus reached (point B). In the meantime, the curing reaction is completed and a cup-like experimental curve is obtained. The time corresponding to OC is the full curing time. The envelope of the experimental curve corresponds to the change of mechanical behavior of the resin system during cure. Since the cup-like experimental curve is symmetric to the time axis, for convenience we can just take the upper-half of the envelope as the isothermal cure curve to analyze the cure process.

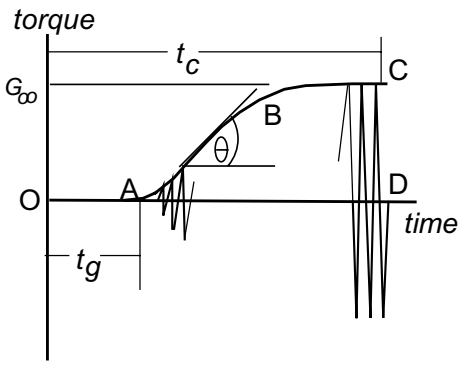


Fig. 2. A typical experimental curve obtained by the dynamic torsional vibration method.

### 2.3. Measurement and characterization

The change of lattice spacing of montmorillonite was measured by using a Rigaku D/max-γB rotating anode X-ray diffractometer with the $CuK_\alpha$ line ($\lambda = 0.1542$ nm), a tube voltage of 40 kV and tube current of 100 mA. The scanning range was from 1.2° to 10° with a rate of 1°/min.

## 3. Results and discussion

### 3.1. X-ray diffraction analysis

The X-ray diffraction patterns for epoxy resin E51/Org-MMT/imidazole composites containing different content of Org-MMT cured under the temperature of 100 °C are shown in Fig. 3. These XRD patterns reveal the change in Org-MMT basal spacing that occurs in the epoxy curing process. For the epoxy resin E51/Org-MMT/imidazole system, it is noteworthy that the (0 0 1) diffraction peak, corresponding to the basal spacing of montmorillonite $d_{001}$, shifted to a lower angle comparable to that of Org-MMT, and the intensity of the peak increased with increased loading of Org-MMT. The X-ray diffraction peak occurs at $2\theta = 4.02°$ for Org-MMT, and for the epoxy resin E51/Org-MMT/imidazole composite the first peak ($n = 1$) and the second peak ($n = 2$) of diffraction appeared at $2\theta = 2.36°$ and 5.27°, respectively. Obviously, the intercalated nanocomposite with the lattice spacing of 37.4 Å (according to $2d \sin\theta = n\lambda$) was obtained. As Pinnavaia [8] pointed out, the lattice spacing of the intercalated nanocomposite increases, but Bragg diffractions still exist in the diffractogram, which shifted to lower angle. If the lattice spacing continues to increase, exfoliated nanocomposite is formed, leading to the disappearance of Bragg diffraction.

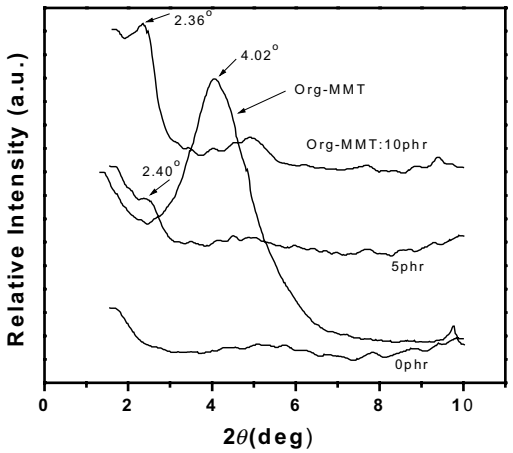


Fig. 3. XRD patterns of epoxy resin E51/Org-MMT/imidazole nanocomposites.

### 3.2. Isothermal cure curve of epoxy resin E51/Org-MMT/imidazole

Fig. 4 shows the isothermal cure curves of the epoxy resin E51/Org-MMT/imidazole composite with Org-MMT loadings of 0, 5 and 10 phr at different temperatures. The curing curves at different temperatures have similar shape, but obvious differences in their gel times $t_g$ and curing rates. It is evident from Fig. 4 that with the increasing temperature the $t_g$ decreases in turn, and the

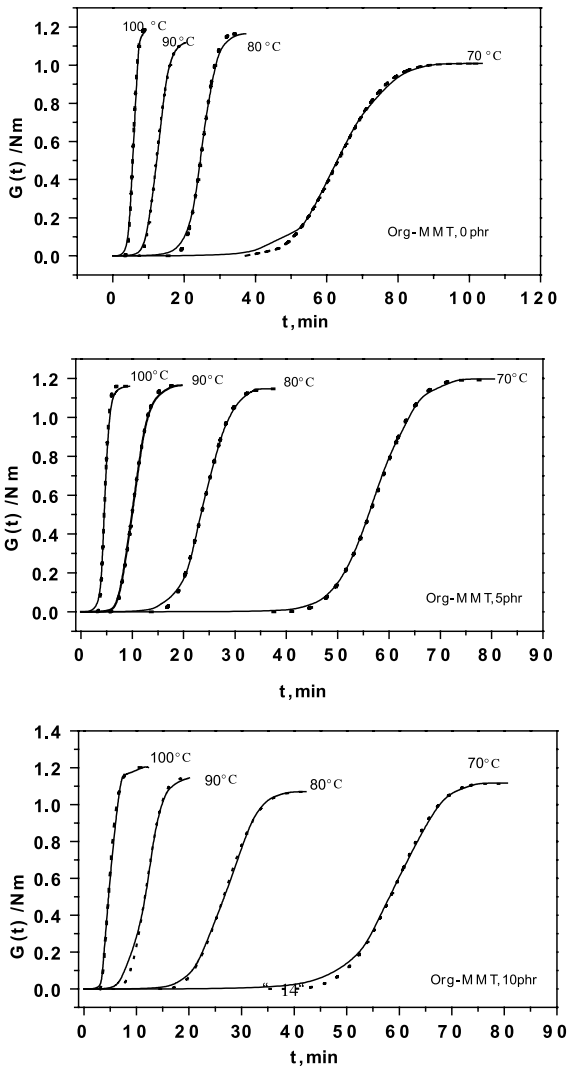


Fig. 4. The isothermal cure curves of torque versus time for epoxy resin E51/imidazole nanocomposites at various temperatures. (—) Experimental; (···) theoretical.

Table 1
Isothermal cure data of epoxy resin E51/Org-MMT/imidazole nanocomposites at different temperature

| Org-MMT (phr) | $T$ (°C) | $t_g$ (min) | $\tau$ (min) | $\tau_0$ ($10^{-13}$ min) | $\beta$ |
|---|---|---|---|---|---|
| 0 | 70 | 37.23 | 29.47 | 13.04 | 2.84 |
| | 80 | 15.17 | 11.11 | | 3.54 |
| | 90 | 7.16 | 6.29 | | 2.36 |
| | 100 | 3.28 | 2.81 | | 2.66 |
| 5 | 70 | 37.37 | 22.62 | 3.67 | 3.62 |
| | 80 | 13.48 | 12.05 | | 3.00 |
| | 90 | 5.64 | 5.49 | | 2.33 |
| | 100 | 3.20 | 1.68 | | 2.38 |
| 10 | 70 | 35.27 | 26.30 | 5.45 | 3.95 |
| | 80 | 14.36 | 14.29 | | 2.95 |
| | 90 | 5.44 | 4.55 | | 3.08 |
| | 100 | 3.07 | 2.28 | | 1.70 |

curing rate is accelerated. The gel time $t_g$ obtained from Fig. 4 and some related data are listed in Table 1.

### 3.3. Theoretical prediction of cure behavior

Hsich's non-equilibrium thermodynamic fluctuation theory [16,17] directly describes the changes of physical or mechanical properties of the curing system during cure. According to the theory, the physical or mechanical properties of the resin system during cure can be expressed as

$$\frac{G_\infty - G(t)}{G_\infty - G_0} = \exp\left[ - \left(\frac{t}{\tau}\right)^\beta \right] \tag{1}$$

where $G_0$ and $G_\infty$ are the initial and final physical and mechanical quantities (torque or modulus, viscosity etc.) during cure, respectively; $G(t)$, the property at time $t$; $\tau$, the time parameter (relaxation time) of the reaction system; and $\beta$, the constant describing the width of the relaxation spectrum. In our experiment the mechanical quantity is torque. As seen from the isothermal cure curve in Fig. 4, $G_0$ is zero, the torque beginning to appear only after the gel time $t_g$. Eq. (1) describing the curing curve after $t_g$ would be

$$\frac{G_\infty - G(t)}{G_\infty} = \exp\left\{ - \left[ \left(\frac{t - t_g}{\tau}\right)^\beta \right] \right\} \tag{2}$$

or

$$G(t) = G_\infty \left\{ 1 - \exp\left[ - ((t - t_g)/\tau)^\beta \right] \right\} \tag{3}$$

Eq. (3) describes the changes in torque of the resin system during cure in which $t_g$ and $G_\infty$ can be read directly from the isothermal cure curve.

In order to obtain the relaxation time $\tau$, let $t = t_g + \tau$, thus

$$G(t = t_g + \tau) = G_\infty(1 - e^{-1}) = 0.63 G_\infty \tag{4}$$

From a measurement of the time corresponding to $0.63G_\infty$ in the experimental curing curve, the relaxation time $\tau$ can be obtained according to $\tau = t - t_g$.

The relationship between the relaxation time $\tau$ and the cure temperature $T$ is in accordance with the Arrhenius equation [14]. Therefore, a straight line can be obtained by plotting $\ln \tau$ versus $1/T$, and the value of $\tau_0$ can be estimated from the intercept of the line as seen in Table 1. The reciprocal of $\tau_0$ is the reflection on the rate of the cure reaction of the system. It is evident that the addition of Org-MMT leads to a decrease in the value of $\tau_0$, that is, increases the value of $1/\tau_0$. Correspondingly, the addition of Org-MMT accelerates the cure rate, which should be the result of introducing a new surface to the reaction system.

Having determined $\tau$, Eq. (3) is reduced to an equation with a single parameter only. A non-linear regression is used to fit Eq. (3) to all experimental cure curves. The values of $\beta$ at various temperatures or Org-MMT loadings can be determined using the line of best fit. With this $\beta$ value, the torque $G(t)$ at any time, i.e., the theoretically predicted value, can be calculated according to Eq. (3) provided that the gel time $t_g$ and the relaxation time $\tau$ are already known. The theoretical curing curves are also plotted in Fig. 4 as a dot line. The theoretical prediction shows a good agreement with the experimental curves for various curing temperatures.

### 3.4. Analysis of curing curve after gel time by the Avrami method

The Avrami theory is most often used to describe the kinetic process of polymer crystallization. Since many molecular aggregates (microgels) or high-molecular-weight particles have been observed during an infinite network formation as a result of crosslinking [18], Lu [19] considered that in a broad sense, crystallization can be considered as a physical form of crosslinking and in

some aspects the behavior of amorphous crosslinking polymers is similar to that of crystals. Therefore it is possible to predict the cure process of thermosets using the Avrami equation. The cure kinetics of the epoxy resin [19,20] and unsaturated polyester [21] have been analyzed with the Avrami equation earlier, and good agreement between theoretical predictions and experimental DSC data was achieved.

The relative degree $\alpha$ of cure at $t$ time can be calculated according to the curing curve as follows

$$\alpha = G(t)/G_\infty \tag{5}$$

and the isothermal curing curves can be changed into the relationship between degree of cure $\alpha$ and curing time $(t - t_g)$ after the gel point, as shown in Fig. 5. The isothermal cure process can be analyzed using the following modified Avrami equation [22]:

$$\alpha = 1 - \exp[-k(t - t_g)^n] \tag{6}$$

or

$$\ln[-\ln(1-\alpha)] = n\ln(t - t_g) + \ln k \tag{7}$$

where $n$ is the Avrami exponent that is a reflection of nucleation and growth mechanisms; and $k$ is a temperature dependent kinetic constant.

The plots of $\ln[-\ln(1-\alpha)]$ versus $\ln(t - t_g)$ for the data obtained on the cure process of epoxy resin E51/Org-MMT/imidazole are shown in Fig. 6. The results

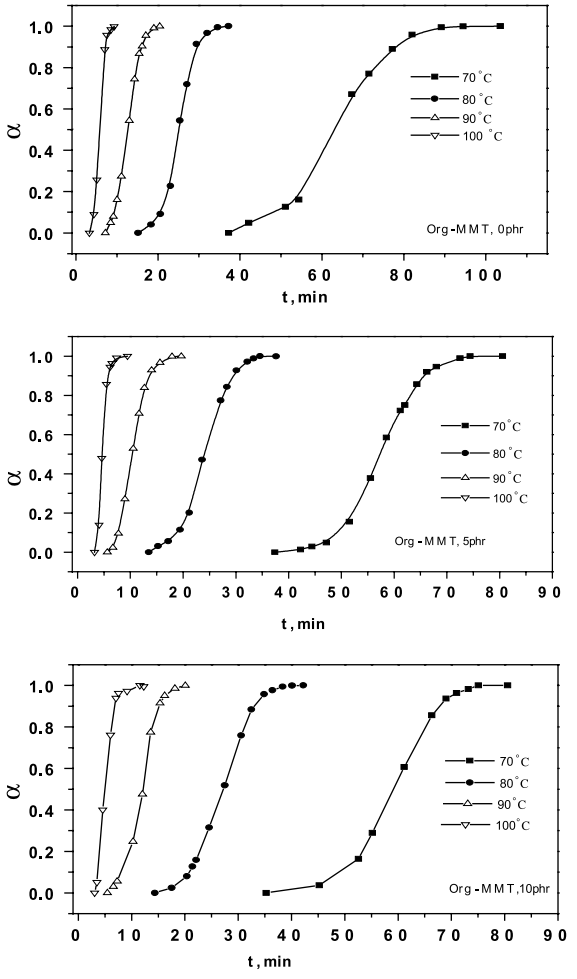


Fig. 5. Degree of cure as a function of cure time for epoxy resin E51/Org-MMT/imidazole nanocomposites at different temperatures and filler loadings.

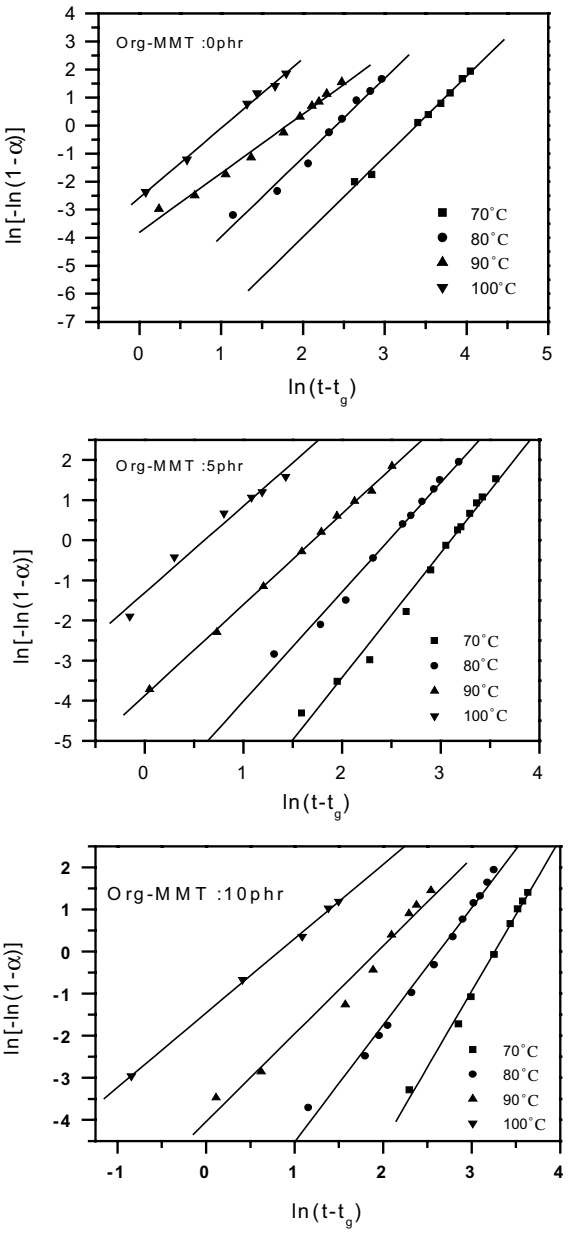


Fig. 6. The Avrami plots of $\ln[-\ln(1-\alpha)]$ versus $\ln(t - t_g)$ of epoxy resin E51/Org-MMT/imidazole nanocomposites.

treated by the Avrami equation are reported in Table 2. The good linearity indicates that it is valid to illustrate the cure process after $t_g$ by the Avrami equation. Meanwhile, it is found that the values of kinetic constant $k$ decreased as the cure temperature increased, that is, the higher temperature, the faster the cure rate, which is in good agreement with the general rule of chemical reactions [23].

The values of the Avrami exponent $n$, describing the isothermal cure, depend on the cure temperatures for epoxy resin E51/Org-MMT/imidazole systems. At lower temperature (<90 °C) the $n$ values are close to around 3 and decreased to ~2 as the temperature increased. Similar results are obtained in epoxy resin E51/imidazole systems without Org-MMT. As we have known, the Avrami exponent provides qualitative information on the nature of the nucleation and the growth processes in the crystallization of a polymer and may be changed. This fact of change in $n$ may imply that a change occurs in the cure mechanism for lower cure temperature, although the formation and growth of microgels (i.e. molecular aggregates) are essentially different from those of crystals [21,24]. After the gel point, the cure reaction is predominantly diffusion controlled, due to the retardation of viscosity, and a mass dispersion limitation eventually sets in, so the microgel particles are forced to impinge on one another, and phase inversion may occur. We may conclude it is less of a mass transfer limitation at a lower cure temperature that leads to the relatively higher value of $n$. The similar result was observed in a zeolite-filled epoxy system by Lu [25].

The half-time of cure, $t_{1/2}$, for experimental and theoretical data by equation $t_{1/2} = (\ln 2/k)^{1/n}$, compared closely in Table 2 for epoxy resin E51/Org-MMT/imidazole systems, confirming the ability of the Avrami equation to represent the isothermal cure process.

The value of the time ($t_p$) at which the maximum rate of cure occurs can be calculated from Eq. (6). When $d^2\alpha/dt^2 = 0$, then obtaining for $t_p$:

$$t_p = \left[\frac{(n-1)}{nk}\right]^{1/n} \tag{8}$$

Values of $t_p$, calculated from Eq. (8), are listed in Table 2 for epoxy resin E51/Org-MMT/imidazole systems, and the shortening of $t_p$ means a faster rate of cure reaction.

### 3.5. Apparent activation energy of the resin system

According to Flory's gelation theory [26], the chemical conversion at the gel point of the resin system is constant and is not related to the reaction temperature and experimental conditions. As a result, the apparent activation energy of the cure reaction $E_a$ can be obtained from the gel time $t_g$

$$\ln t_g = C + E_a/RT \tag{9}$$

where $T$ is the curing temperature (K); $R$, the gas constant, and $C$, a constant. Fig. 7 shows a plot of $\ln t_g$ versus $1/T$ for various Org-MMT loadings of 0, 5 and 10 phr. The apparent activation energy $E_a$ can be calculated from the slope of the lines.

The activation energy can also be estimated by the Avrami method. An empirical approach can be used to describe the temperature dependence of the kinetic constant $k$. Assuming that $k$ is thermally activated [27]:

$$k^{1/n} = k_0 \exp(-E_a/RT) \tag{10}$$

where $E_a$ is an activation energy associated with the cure process and $k_0$, a pre-exponential constant. The

Table 2
Values of isothermal curing process of epoxy resin E51/Org-MMT/imidazole nanocomposites

| Org-MMT (phr) | $T$ (°C) | $t_g$ (min) | $t_{1/2}$ (min) | $t^*_{1/2}$ (min) | $t_p$ (min) | $k$ | $n$ |
|---|---|---|---|---|---|---|---|
| 0 | 70 | 37.23 | 26.13 | 25.87 | 25.29 | $6.315 \times 10^{-5}$ | 2.86 |
| | 80 | 15.17 | 10.03 | 9.78 | 9.53 | $1.118 \times 10^{-3}$ | 2.82 |
| | 90 | 7.16 | 5.53 | 5.10 | 4.48 | $2.226 \times 10^{-2}$ | 2.11 |
| | 100 | 3.28 | 2.40 | 2.43 | 2.29 | $7.610 \times 10^{-2}$ | 2.48 |
| 5 | 70 | 37.37 | 20.04 | 19.50 | 19.36 | $6.745 \times 10^{-5}$ | 3.11 |
| | 80 | 13.48 | 10.51 | 10.33 | 10.00 | $1.180 \times 10^{-3}$ | 2.73 |
| | 90 | 5.64 | 4.76 | 4.69 | 4.27 | $2.075 \times 10^{-2}$ | 2.27 |
| | 100 | 3.20 | 1.56 | 1.54 | 1.38 | $2.696 \times 10^{-1}$ | 2.16 |
| 10 | 70 | 35.27 | 23.95 | 23.44 | 23.72 | $7.618 \times 10^{-6}$ | 3.62 |
| | 80 | 14.36 | 13.09 | 12.12 | 11.78 | $6.735 \times 10^{-4}$ | 2.78 |
| | 90 | 5.44 | 6.63 | 5.80 | 5.06 | $1.758 \times 10^{-2}$ | 2.09 |
| | 100 | 3.07 | 1.82 | 1.85 | 1.42 | $2.327 \times 10^{-1}$ | 1.77 |

*Obtained by the equation $t_{1/2} = (\ln 2/k)^{1/n}$

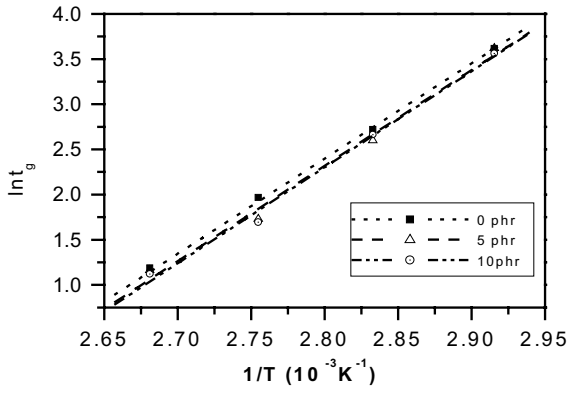


Fig. 7. Plots of $\ln t_g$ versus $1/T$ of epoxy resin E51/Org-MMT/imidazole nanocomposites.

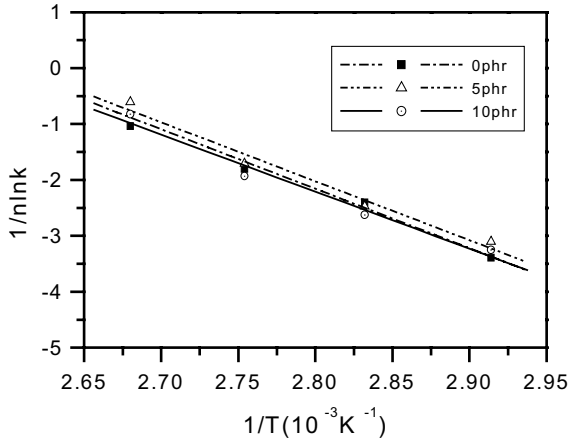


Fig. 8. Plots of $1/n \ln k$ versus $1/T$ of epoxy resin E51/Org-MMT/imidazole nanocomposites.

logarithmic plots of $(1/n)\ln k$ as a function of $1/T$ are shown in Fig. 8 for epoxy resin E51/Org-MMT/imidazole systems. The good fit to linearity allows calculation of the activation energy from the slope of the straight line.

The values of activation energy obtained by the above methods are listed in Table 3. From Table 3 it can be seen that the activation energies obtained by the two methods are very close, whether for the cure system with or without Org-MMT. Values of $E_a$ obtained from Flory's theory for the epoxy resin E51/Org-MMT/imidazole and epoxy resin/imidazole system have a nearly constant value of 88 kJ/mol, which is identical to our DSC study and our other published $E_a$ values of 69 kJ/mol [28] and 80.3 kJ/mol [29] respectively. A similar result is observed according to the Avrami equation. The addition of Org-MMT to epoxy resin E51/imidazole systems has an insignificant effect on the activation energy, indicating that the addition of Org-MMT has no change on the mechanism of the cure reaction. This fact is in accordance with the other results [30,31].

Table 3
Activation energy of epoxy resin E51/Org-MMT/imidazole nanocomposites

| Org-MMT (phr) | $E_{a1}$ (kJ/mol) | $E_{a2}$ (kJ/mol) |
|---|---|---|
| 0 | 87.6 | 88.3 |
| 5 | 87.9 | 87.6 |
| 10 | 88.4 | 84.8 |

$E_{a1}$, obtained by Eq. (9) $E_{a2}$, obtained by Eq. (10).

## 4. Conclusion

The isothermal cure behavior of epoxy resin E51/Org-MMT/imidazole intercalated nanocomposites was investigated by a dynamic torsional vibration method. The Flory's gelation theory, a non-equilibrium thermodynamic fluctuation theory and the Avrami equation have been used to predict the gel time $t_g$ and the cure behavior of epoxy resin/Org-MMT/imidazole systems with different Org-MMT loadings at various temperatures. The theoretical prediction is in good agreement with the experimental results. The addition of Org-MMT reduces the gel time $t_g$ and increases the cure rate, the value of $k$, and half-time $t_{1/2}$ of cure after gelation point decreases with increasing cure temperature, and the Avrami value of $n$ is around 3 when the temperature is lower than 90 °C, but it drops to ~2 above 90 °C. The addition of Org-MMT has little effect on the apparent activation energy of the cure reaction. Compared to the cure process of epoxy resin/imidazole in the presence or absence of Org-MMT, no special curing process is required for the formation of epoxy resin/Org-MMT/imidazole intercalated nanocomposite.

## Acknowledgement

The authors gratefully acknowledge the financial support from the Nature Science Foundation of Anhui Province, China.

## References

[1] Kornmann X, Lindberg H, Berglund LA. Polymer 2001; 42:1303.
[2] Kornmann X, Lindberg H, Berglund LA. Polymer 2001; 42:4493.
[3] Hsiue GH, Liu YL, Liao HH. J Polym Sci, Part A: Polym Chem 2001;39:986–96.
[4] Bhattacharrya SK, Tummala RR. Microelectron J 2001; 32:11–9.

[5] Messersmith PB, Giannelis EP. Chem Mater 1994;6:1719.
[6] Lan T, Pinnavaia TJ. Chem Mater 1994;6:2216.
[7] Lan T, Kaviratna PD, Pinnavaia TJ. Proc ACS Div Polym Mater Sci Eng 1994;71:528.
[8] Lan T, Kaviratna PD, Pinnavaia TJ. Chem Mater 1995; 7:2144.
[9] Chin IJ, Thurn-Albrecht T, Kim HC, Russell TP, Wang J. Polymer 2001;42:5947.
[10] Stevens GC. J Appl Polym Sci 1981;26:4279.
[11] Sacher E. Polymer 1973;14:19.
[12] Wang MW, Lee CT, Lin MS. Polym Int 1997;44:503.
[13] He PS, Li CE. J Appl Polym Sci 1991;43:1011.
[14] He PS, Li CE. J Mater Sci 1989;24:2951.
[15] Xu WB, He PS. Chinese Appl Chem 2001;18:469.
[16] Hsich HS-Y. J Mater Sci 1978;13:2560.
[17] Hsich HS-Y. J Appl Polym Sci 1982;27:3265.
[18] Pollard M, Kardos JL. Polym Eng Sci 1987;27:829.
[19] Lu MG, Shim MJ, Kim SW. Mater Sci Commun 1998; 56:193.
[20] Kim SW, Lu MG, Shim MJ. Polym J 1998;30:90.
[21] Lu MG, Shim MJ, Kim SW. Thermochim Acta 1998; 323:37.
[22] Liu SL, Chung TS, Yamaguchi A. J Polym Sci, Part B: Polym Phys 1998;36:1679.
[23] Smiitzis J, Stamboulis A, Tsoros D, Martakis N. Polym Int 1997;43:380.
[24] Lu MG, Shim MJ, Kim SW. J Therm Anal Calorim 1999; 58:701.
[25] Lu MG, Shim SW, Kim SW. Polym Eng Sci 1999;39:274.
[26] Flory PJ. Principles of polymer chemistry. New York: Cornell University Press; 1953. 353.
[27] Peggy C, Su-Don H. Polymer 1986;27:1183.
[28] Xu WB. Polymer/montmorillonite intercalated nanocomposite. Doctoral dissertation, University of Science and Technology Press, Hefei, 2001.
[29] Berger J, Lohse F. J Appl Polym Sci 1985;30:531.
[30] Ryan ME, Dutta A. Polymer 1979;20:203.
[31] Ng H, Manas-Zloczower I. Polym Eng Sci 1989;29:302.